Automated Assessment of Keratocyte Density in Stromal Images from the ConfoScan 4 Confocal Microscope

Jay W. McLaren, William M. Bourne, and Sanjay V. Patel

Purpose. To develop a program to determine cell densities in images from the ConfoScan 4 (Nidek, Inc., Freemont, CA) confocal microscope and compare the densities with those determined in images obtained by the Tandem Scanning confocal microscope (Tandem Scanning Corp., Reston, VA).

Methods. A program was developed that used image-processing routines to identify stromal cell nuclei in images from the ConfoScan 4 confocal microscope. Cell selection parameters were set to match cell densities from the program with those determined manually in 15 normal corneas of 15 volunteers. The program was tested on scans from 16 other normal volunteers and 17 volunteers 3 years after LASIK. Cell densities were compared to densities determined by manual assessment and to those in scans by the Tandem Scanning confocal microscope in the same corneas.

Results. The difference in cell density between the automatic and manual assessment was -539 ± 3005 cells/mm^3 (mean $\pm$ SD, $P = 0.11$) in the 16 test corneas. Densities estimated from the ConfoScan 4 agreed with those from the Tandem Scanning confocal microscope in all regions of the stroma except in the anterior 10%, where the ConfoScan 4 indicated a 30% lower density.

Conclusions. Differences in anterior stromal cell density between the ConfoScan 4 and the Tandem Scanning confocal microscope can be explained by the different optical designs. The lower spatial resolution of the ConfoScan 4 limits its ability to resolve thin layers. The adaptation of our earlier cell-counting program to the ConfoScan 4 provides a timesaving, objective, and reproducible means of determining stromal cell densities in images from the ConfoScan 4. (*Invest Ophthalmol Vis Sci.* 2010;51:1918–1926) DOI:10.1167/iovs.09-4186

Keratocytes are fibroblast-like cells that maintain the health and clarity of the corneal stroma. Their density is highest in the anterior stroma and is relatively uniform in the central and posterior stroma,[1,2] although some investigators have noted an increased density in the posterior stroma.[1] The overall density of keratocytes decreases slowly with age.[1–5] Investigators have studied changes in keratocyte density in a variety of conditions, including contact lens wear,[6–11] keratoconus,[12–15] excimer laser keratorefractive surgery,[16–20] and corneal transplantation.[21–24] Decreased keratocyte density has been associated with increased corneal backscatter after penetrating keratoplasty,[25] although a causal relationship has not yet been established. The minimum number of keratocytes necessary to maintain a healthy cornea is unknown, particularly in the anterior stroma where densities are highest. Knowing keratocyte density is critical to understanding how these cells behave, their importance in recovery after surgical intervention, and how they maintain a clear corneal stroma. The accuracy and precision of measuring cell density are influenced by the optical parameters of the instrument for recording images of the corneal stroma, as well as the methods used to identify and count cells in these images.

Confocal microscopy has provided a convenient and noninvasive method of examining keratocytes and other corneal cells and structures.[26,27] A confocal scan (a series of images at known progressive depths) through the entire thickness of the cornea is noninvasive, provides a record of structure with depth, and provides images that can be used to determine cell density and other morphologic variables. Keratocyte nuclei appear as bright objects in stromal images. Although these bright objects are usually associated with keratocytes, images are nonspecific for cell type; an observer cannot discriminate between keratocytes, bone marrow-derived cells, and other cells that have bright nuclei.[28–31] Cell density is typically determined by counting the number of nuclei in a predefined area of the image and dividing this number by the volume represented by the optical section of the image, although some investigators present cell density as cells per unit area of the image. Although simple in concept, counting cells is time consuming and subjective and is hindered by high intra- and interobserver variation.[32] Cell densities determined in different studies with different instruments can be compared with each other only if spatial dimensions used to estimate density are properly calibrated for each microscope.

A few objective automated methods have been developed that use image-processing technology to identify and count cell nuclei in confocal images, and these methods are repeatable and require much less analysis time than do manual methods.[32–34] Image-processing programs developed for a particular microscope cannot be directly applied to images from other microscopes because the optical properties of each microscope uniquely affect the cell selection criteria of the program. For example, the ConfoScan 4 (Nidek Technologies, Inc., Padova, Italy) provides images of keratocyte nuclei with higher contrast, a greater depth of field, and a more variable field brightness from the center to the edges than do images from the Tandem Scanning confocal microscope (Tandem Scanning Corp., Reston, VA). When images from the ConfoScan 4 were assessed with analysis programs developed for the Tandem Scanning microscope, the cell densities did not match those in the manual assessment. A program that assesses stromal cell density in images from the ConfoScan 4 or other confocal microscopes would be valuable. The Tandem Scanning confo-

From the Department of Ophthalmology, Mayo Clinic, Rochester, Minnesota.

Presented at the annual meeting of the Association for Research in Vision and Ophthalmology, Fort Lauderdale, Florida, May, 2008.

Supported in part by National Institutes of Health Grant EY02037 (WMB); an unrestricted departmental grant from Research to Prevent Blindness (RPB), Inc., New York, NY; and the Mayo Foundation, Rochester, MN. SVP is an RPB Olga Keith Wiess Special Scholar.

Submitted for publication June 19, 2009; revised September 10, 2009; accepted October 20, 2009.

Disclosure: **J.W. McLaren**, None; **W.M. Bourne**, None; **S.V. Patel**, None

Corresponding author: Jay W. McLaren, Mayo Clinic, 200 First Street SW, Rochester, MN 55905; mclaren.jay@mayo.edu.

cal microscope is no longer available, and many investigators now use newer microscopes in studies of stromal cells.

In this study, we developed a new program to determine cell density in images from the ConfoScan 4. The program was adjusted to emulate a human observer by using a sample of 15 normal corneas and was tested on another sample of 16 normal corneas and 33 corneas of 17 patients 3 years after laser in situ keratomileusis (LASIK). We also compared cell densities determined from confocal images recorded by the ConfoScan 4 with those from images recorded by the Tandem Scanning confocal microscope, and we will discuss the differences in cell density in the anterior stroma in terms of the unique optical characteristics of each confocal microscope.

Methods

Subjects

All subjects were normal control participants in other studies in our laboratory[35,36] and were examined by slit lamp biomicroscopy to assure that their corneas and anterior segments were normal. Image variables used to identify the cells were determined from confocal images of 15 corneas of 15 subjects, and the program was tested on a separate group of 16 corneas of 16 subjects. Confocal images were examined from an additional 33 corneas of 17 patients 3 years after LASIK. These patients were part of another study[36] that examined the effect of LASIK on the cornea. Each subject gave informed consent to participate after discussing the nature and possible consequences of the study. All studies were approved by the Institutional Review Board of Mayo Clinic and conformed to the tenets of the Declaration of Helsinki for research involving human subjects.

Confocal Microscopy

Corneas were scanned with a ConfoScan 4 scanning-slit confocal microscope with a *z*-ring adapter, as described elsewhere.[35] Briefly, the cornea was anesthetized by instillation of topical proparacaine 0.5%. The tip of the objective lens and *z*-ring were coated with a viscous contact solution (GenTeal Gel; Novartis Ophthalmics, East Hanover, NJ), and the objective was advanced until the solution contacted the cornea. The operator adjusted the position of the lens until the field of view of the microscope was centered on the bright reflex from the endothelium and then pressed a button to initiate a scan. Under scanner control, the *z*-ring contacted the cornea, and the focal plane advanced to approximately 100 μm posterior to the endothelium before reversing direction and scanning anteriorly at a fixed rate. After advancing past the anterior surface of the cornea, the microscope moved the focal plane to the initial position and repeated the scan. Two passes through the cornea were recorded. The step distance between frames was set to 4.0 μm and the lamp intensity was set to 90%. The pressure setting of the *z*-ring on the cornea was 20 (this instrument parameter has no units but determines the force on the *z*-ring needed to maintain contact with the cornea). The microscope recorded 350 frames at 25 frames per second. Video sequences were exported from the operating program as audio-video interleave (avi) files for image processing.

The second group of 16 corneas was scanned by the ConfoScan 4, as just described, and by the Tandem Scanning confocal microscope by methods that have been published.[2,33] The focal plane of this microscope was advanced in an anterior-to-posterior direction through the cornea at approximately 72 μm/s (approximately a 2.4-μm step),[37] and images were stored by a computer at 30 frames/s. The video camera automatically adjusted its gain to maintain constant image brightness.

The 33 corneas that had undergone LASIK were examined by both the ConfoScan 4 and the Tandem Scanning confocal microscopes by using the same recording variables as used with the other participants. These corneas provided an example of tissue that was not entirely normal. In previous studies, we and others have shown a decreased cell density in the anterior stroma after LASIK.[18,20,38,39]

Selection of Frames and Manual Assessment of Cell Density

From each scan by the ConfoScan 4 and Tandem Scanning microscope, 10 frames from the stroma were selected manually that had nonblurred images of cell nuclei and did not have signs of motion artifact. Images were selected from the first pass by the ConfoScan 4, unless the first pass did not contain enough high-quality frames or showed obvious signs of movement artifacts. Two frames were selected in each of five layers of the stroma: the anterior 0% to 10%, 10% to 33%, 33% to 66%, 66% to 90%, and 90% to 100% of stromal depth.[11] In the anterior 10%, the first frame selected was always the most anterior clear frame that contained stromal cells. Frames in the posterior stroma were selected far enough anterior to the endothelium that they excluded superposed images of endothelial cells.

In each selected video frame, an observer counted bright objects, presumed to represent keratocyte nuclei, inside a predefined rectangle by using a simple point-and-click method, with a marker placed on each object to prevent double counting. Objects that touched the bottom or left edge of the rectangle were counted, but objects that touched the top or right edge were not. Frames from each cornea were presented in random order for cell counting so that the investigator was masked to the depth of the frame in the stroma. Cell density was expressed as cells per cubic millimeter:

$$\text{Density} = \frac{N}{A\delta} \qquad (1)$$

where N is the number of objects counted, A is the area of the selection rectangle, and δ is the effective depth of field. The area A was determined by a rectangle 212 $\times$ 238 μm (horizontal $\times$ vertical) in images from the ConfoScan 4, and 379 $\times$ 286 μm in images from the Tandem Scanning microscope. The distance between pixels was determined from scans of a scale with etched lines spaced by 100 μm.

We assumed δ = 11.9 μm in images from the Tandem Scanning microscope.[40] The depth of field of the ConfoScan 4, was determined from the brightness profile of a scan through the surface of a glass plate, with the intensity of the lamp reduced to between 25% and 42% of maximum to prevent saturation of the camera. The brightness curve through a reflecting surface shows an estimate of the spread of a point because of depth of field in the axial direction (point-spread function), and the width of this brightness curve at half of the maximum brightness has been used to estimate the depth of field.[33,40–42] To this width, we added the presumed depth of a typical cell (assumed to be 1 μm) to account for cells that are partially visible at the anterior and posterior edges of the field.[33,42] The width of the brightness curve at half of the maximum intensity plus the presumed depth of a typical cell (assumed to be 1 μm) was used as the effective depth of field.

Automated Assessment of Cell Density

A program that was developed to assess cell density in images from the Tandem Scanning microscope, described in detail previously,[32] was modified in two ways to process images from the ConfoScan 4. The first modification corrected the high brightness inhomogeneity across the field of the ConfoScan 4 images (Fig. 1), by subtracting from each stromal image an image of a uniformly scattering standard solution (AMCO Clear; GFS Chemicals, Columbus, OH), diluted to a concentration of 500 NTU (nephelometric turbidity units). The image of the solution was scaled so that the mean intensity in a central rectangle (60 $\times$ 200 pixels) was equal to the mean intensity of the stromal image in the same area. A constant offset equal to 100 was then added to the intensity of each pixel of the difference image, and the result was converted to a binary image by use of a threshold. Further processing steps, identical with those described earlier,[32] were used to identify bright objects. As a second change, a new relationship was identified between the field brightness (I_{im}) and the optimum brightness-area-product threshold (BAP_{thr}) used to select the bright objects that most

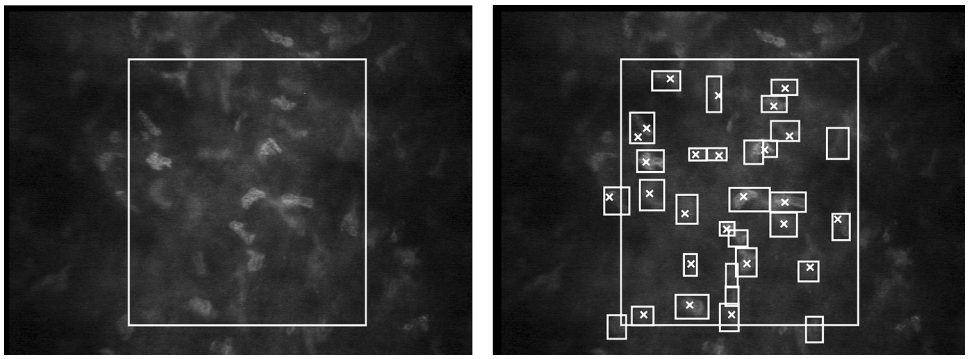

FIGURE 1. Image of normal midstroma recorded with ConfoScan 4. *Left*: the brightness of the field decreased considerably outside the rectangular area used to assess cell density. *Right*: ×, each object identified manually by an observer as a cell nucleus; *rectangles*: each object identified by the program as a cell. Cells that overlapped the *left* or *bottom* boundary were counted, whereas the cells that touched the *right* or *top* boundary were not. In this frame, the program selected more objects as cells than the observer did, although in some frames the program selected fewer.

likely represented cells. The relationship was based on a linear model when brightness was below a transition intensity, and a constant when brightness was above this intensity:

$$BAP_{thr} = \begin{cases} I_{im}m+b & I_{im} \leq I_{tr} \\ BAP_{max} & I_{im} > I_{tr} \end{cases} \quad (2)$$

where m and b are constants, I_{tr} is the transition brightness and is equal to $(BAP_{max} - b)/m$, and BAP_{max} is the maximum threshold when field brightness is greater than I_{tr}. The coefficients m and b were determined by the method of least squares to minimize the difference between automated and manual cell density assessment in the 15 corneas that were assessed by both methods. The constant BAP_{max} was the mean of the optimum BAP_{thr} when I_{im} was greater than I_{tr}.

Cell Density in Test Subjects

The automated method was used to assess cell density in 10 frames from each of 16 corneas of 16 subjects who were different from those used to determine the selection coefficients in equation 2. Cell density was determined manually in the same frames, and differences between the manual and automatic methods and the limits of agreement were calculated as described by Bland and Altman.[43] Limits of agreement are the mean difference ± 2 SD of the difference. This range includes approximately 95% of the differences between methods and provides a method of assessing how well two measurements of the same variable agree.

Cell densities determined from images by the ConfoScan 4 (automated method) were also compared to densities determined in the same corneas on the same day from scans by the Tandem Scanning confocal microscope. Frames were selected from the same regions of stroma identified in scans from the ConfoScan 4, and the automated program designed for the Tandem Scanning microscope was used to determine cell density in these images.[32] Differences in cell densities in each layer between microscopes were examined by using paired *t*-tests.

Cell Density in Corneas after LASIK

In the corneas that had undergone LASIK, two frames were selected from each of six layers, as described by Mitooka et al.[39] The LASIK interface was identified based on appearance of bright particles, and the stroma anterior to this (LASIK flap) was divided into two equally thick layers. The 100-μm layer immediately posterior to the interface (retroablation zone) was subdivided into anterior and posterior halves, and the posterior 66% to 90% and 90% to 100%, based on preoperative corneal thicknesses, were also considered. Two frames were selected from each of these regions in images from each microscope. Cell densities were determined by using the respective automated method for each confocal microscope. We compared density between frames in the anterior half of the LASIK flap and in the remaining regions between the two microscopes by using generalized estimating equation (GEE) models to account for possible correlation between measurements from fellow eyes of the same subject. The significance of differences between the five deeper layers were Bonferroni-corrected for five comparisons. We also used GEE models to compare mean density in the anterior flap with density in the anterior 10% of the stroma of the 16 normal corneas and to compare the posterior flap and anterior retroablation zone with analogous layers in the normal corneas.

Comparison of Cell Density Profiles in the Anterior Stroma

In a subset of 11 corneas scanned by both instruments, the respective programs determined cell density in every frame from the subbasal nerve layer to the endothelium. The depth of each frame was expressed as a percent of stromal thickness, and each scan was shifted so that the peak cell densities in the anterior stroma were aligned. The mean maximum and the position of the cell density peak in scans from the ConfoScan 4 were compared with those from the Tandem Scanning confocal microscope.

RESULTS

The brightness of confocal images recorded by the ConfoScan 4 was greatest at the center and diminished considerably toward the sides of the field (Fig. 1, left). The selection rectangle and bright objects identified as cells are indicated in a typical image (Fig. 1, right). Not all the cells identified by the observer were selected by the program, and in some cases the program selected objects that were not identified by the observer. The full-width-at-half-maximum of a scan through a reflecting surface was 24.4 ± 0.9 μm ($n = 4$), and with the addition of 1 μm for the assumed thickness of a keratocyte nucleus,[33] the depth of field, δ, in equation 1 was 25.4 μm. The program took approximately 10 seconds to assess each frame, whereas manual assessment took approximately 60 seconds per frame.

Selection Parameters

The average BAP_{thr} increased with field brightness, I_{im}, when the average field intensity was below 40 iu (intensity units, Fig. 2). The coefficients of equation 2 were $m = 149.3$ pixel^2 and $b = 3118$ iu pixel^2 when I_{im} was less than 40 iu, and BAP_{max} was 9439 iu pixel^2.

The most anterior frames behaved somewhat differently than the deeper frames and required a lower maximum threshold to match densities determined manually. In frames that were within 25 μm of the most anterior frame that contained cell nuclei, the BAP_{max} was 7251 iu pixel^2.

Cell Density in Corneas Used to Define Selection Coefficients

Mean cell density determined manually and automatically in each of the five layers from the scans used to define the BAP_{thr} are given in Table 1, and mean density in each of the 10 frames

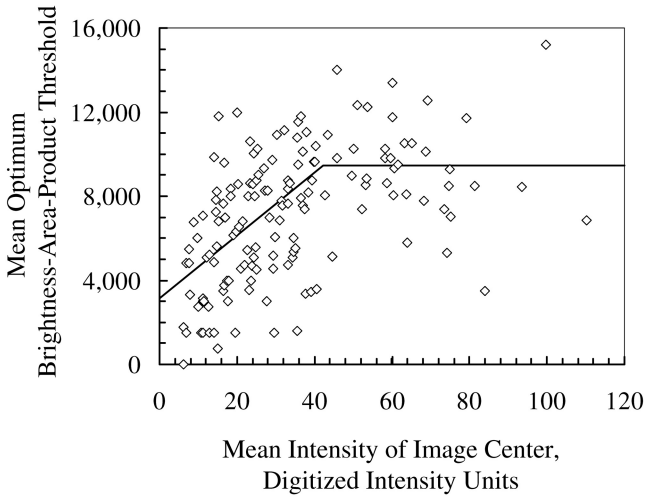

FIGURE 2. The BAP_{thr} for identifying cells from objects in each frame changed as image intensity increased. Each marker represents the optimum BAP_{thr}, which forced the cell density determined automatically to be equal to that determined manually. The fitted line, determined by the least-squares method when intensity was below 40 and by a simple mean when intensity was above 40, was used to determine the BAP_{thr} within each frame.

selected is illustrated in Figure 3. The unweighted mean difference between manual and automatic assessment was −110 ± 3374 cells/mm^3, or 0.5% of the mean density ($P = 0.8$). Limits of agreement were −6857 to 6637 cells/mm^3.

Cell Density in Test Corneas

In the 16 test corneas not used to determine selection criteria, cell density was not significantly different between the methods ($P > 0.3$) in all except the central third (Table 2). Cell density was underestimated in this region by 1520 ± 2172 cells/mm^3 ($P = 0.014$). The mean difference between manual and automatic assessment of all frames examined was −549 ± 3893 cells/mm^3 ($P = 0.11$, $n = 160$ frames); the limits of agreement were −8336 to 7238 cells/mm^3 (Fig. 4).

Differences between the ConfoScan 4 and Tandem Scanning Microscopes

In the anterior 10% of stroma adjacent to Bowman's layer, the mean cell density determined from images recorded by the ConfoScan 4 was 31,677 ± 4,886 cells/mm^3, whereas the mean density from the Tandem Scanning confocal microscope was 44,126 ± 6,680 cells/mm^3 ($P < 0.001$), both determined by the automated method. In all deeper layers, the densities were not significantly different between the two instruments ($P > 0.18$, Table 2, Fig. 5).

TABLE 1. Cell Densities in Five Layers of 15 Normal Corneas Determined by Automatic and Manual Methods in the Same ConfoScan 4 Images

Stromal Layer	Automatic	Manual	Difference
Anterior 10%	31,644 ± 5,279	32,062 ± 5,230	−418 ± 4,309
10%–33%	26,021 ± 2,506	25,289 ± 3,564	732 ± 2,840
33%–66%	24,164 ± 4,177	24,400 ± 3,506	−236 ± 2,546
66%–90%	24,687 ± 4,489	24,766 ± 3,419	−79 ± 3,336
90%–100%	24,504 ± 4,594	25,054 ± 3,071	−549 ± 3,852
Unweighted mean $n = 75$ layers	26,204 ± 5,046	26,314 ± 4,729	−110 ± 3,374

Cell density is expressed as mean cells per cubic millimeter ± SD. These densities were used to determine selection parameters for the cell-counting program. Differences between the automatic and manual methods were not significant ($P > 0.3$).

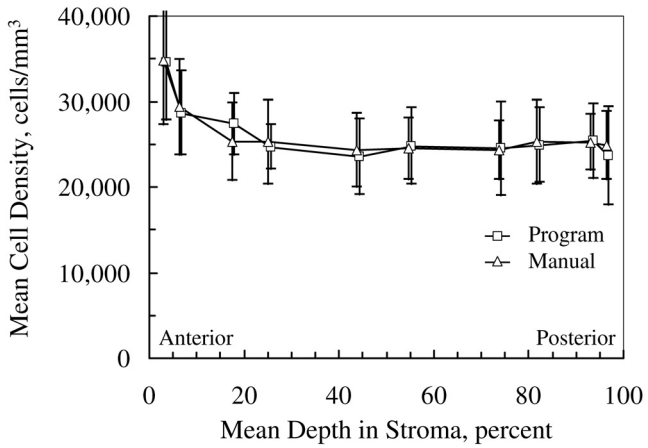

FIGURE 3. Mean cell density in 15 corneas used to determine selection criteria in images from the ConfoScan 4. The markers have been offset slightly for clarity. Error bars, ± SD

The mean cell density profile, after alignment on the frame with the greatest cell density, demonstrated a higher and sharper peak in scans from the Tandem Scanning confocal microscope than in scans from the ConfoScan 4 (Fig. 6). Mean peak cell density in 11 corneas was 33,308 ± 6,141 cells/mm^3 in the scans from the ConfoScan 4 and 57,266 ± 10,767 cells/mm^3 in the scans from the Tandem Scanning microscope ($P < 0.001$). The average depth of the peak was 8.4% of the stromal thickness in scans from the ConfoScan 4, whereas it was 3.5% of stromal thickness with the Tandem Scanning microscope.

Cell Density in Corneas after LASIK

Three years after LASIK, cell density in the anterior flap was estimated to be 29,718 ± 4,162 cells/mm^3 by the ConfoScan 4 and 35,089 ± 6,207 cells/mm^3 by the Tandem Scanning confocal microscope ($P < 0.001$, $n = 33$ corneas). The cell density in this region was not significantly different from the density in the anterior 10% of the stroma in the control corneas, as estimated by the ConfoScan 4 ($P = 0.18$), whereas the density estimated by the Tandem Scanning microscope in this region was significantly less than that in the controls estimated with the same instrument ($P < 0.001$). Mean cell density in deeper layers was 21,953 ± 4,130 cells/mm^3 by the ConfoScan 4 and 21,355 ± 4,710 cells/mm^3 by the Tandem Scanning confocal microscope; the difference between instruments was not significant ($P > 0.16$).

Cell density in the posterior flap and anterior retroablation zone were 22,027 ± 4,234 and 20,613 ± 4,076 cells/mm^3, respectively, with the ConfoScan 4, and 21,464 ± 5,131 and 22,177 ± 4,203 cells/mm^3, respectively, with the Tandem Scanning microscope. These densities were not significantly different between instruments ($P > 0.1$) but were significantly less than those in the corresponding regions of the normal corneas, 10% to 33% of stromal thickness, as given in Table 2 ($P < 0.001$).

DISCUSSION

This program provides a valuable, objective tool for assessing cell density in stromal images from the ConfoScan 4, a clinical confocal microscope. It saves time and is repeatable, whereas manual assessment is labor intensive and subject to the inter-

Table 2. Cell Densities Measured by the ConfoScan 4 and Tandem Scanning Confocal Microscopes in 16 Corneas

	ConfoScan 4			TSCM	
Stromal Layer	Automatic	Manual	Difference Auto − Manual	Automatic	Difference TSCM − ConfoScan 4
Anterior 10%	31,677 ± 4,886	31,358 ± 5,506	319 ± 4,009	44,126 ± 6,680	12,449 ± 8,326*
10%–33%	25,890 ± 3,517	26,062 ± 4,046	−172 ± 2,695	27,582 ± 4,553	1,692 ± 4,843
33%–66%	24,419 ± 3,498	25,939 ± 2,828	−1,520 ± 2,172†	23,317 ± 5,043	−1,103 ± 6,107
66%–90%	24,493 ± 3,092	24,983 ± 2,171	−490 ± 2,765	24,498 ± 3,475	5 ± 5,433
90%–100%	22,728 ± 4,930	23,610 ± 3,096	−883 ± 3,418	23,230 ± 4,798	502 ± 7,506
Unweighted mean, n = 80 layers	25,841 ± 5,027	26,391 ± 4,486	−549 ± 3,065	24,647 ± 4,661	2,709 ± 8,114* 274 ± 5,994‡

Cell densities are expressed as the mean cells per cubic millimeter ± SD. These corneas were independent of corneas used to determine selection criteria for the automatic method. The differences were not significant ($P > 0.1$), except where indicated. TSCM, Tandem Scanning confocal microscope.

* ConfoScan 4 significantly different from TSCM, $P < 0.001$, paired *t*-test.

† Automatic significantly different from manual, $P = 0.014$, paired *t*-test.

‡ Mean difference between 10% and 100% stromal thickness.

pretation of the observer. This program will be valuable in longitudinal studies of corneas before and after surgical or medical treatments and should reduce inter- and intraobserver variations in estimates of cell density. Long-term studies should not be affected by variations in subjective cell selection, provided the image quality of the confocal microscope remains consistent.

Two adjustments were necessary to adapt the original program, designed for the Tandem Scanning confocal microscope, for use with the ConfoScan 4. First, image brightness varied greatly across the field of the ConfoScan 4 and was homogenized by subtracting an intensity-scaled image of a uniformly scattering solution (AMCO Clear; GFS Chemicals) from the stromal images. Second, a new relationship was empirically defined between image brightness and the optimum BAP_{thr} and was used to select objects that most likely represented cells. Similar modifications should be considered when programs that assess images are adapted for use with any new confocal microscope design, because of the different image characteristics from instrument to instrument.

Differences between the ConfoScan 4 and the Tandem Scanning Confocal Microscope

Other than in the anterior 10% of the stroma, cell densities determined with the ConfoScan 4 were similar to the densities determined with the Tandem Scanning microscope, consistent with earlier comparisons between the ConfoScan 3 and the Tandem Scanning microscope.[40] In the deeper layers, the cells are uniformly distributed through the depth of field (Fig. 7, right), and even though depths of field and the number of cells counted per unit area were unequal between the microscopes, the estimates of density from equation 2 were similar.

In the anterior 10% of the stroma, estimates of the cell densities were considerably lower in images from the ConfoScan 4 than they were with the Tandem Scanning confocal microscope. This difference can be explained by the variation in depth of field (δ in equation 2) and in the number of cells included in this field at the anterior boundary. Images of the anterior boundary of the stroma suggest that a high concentration of keratocyte nuclei inhabit a thin layer just beneath Bowman's layer, and this profile is consistent with previous observations.[2] Cell density decreases rapidly posterior to this layer, and no cells lie anterior to the boundary. When the most anterior cells are in clear focus with the ConfoScan 4, which has an approximately 26-μm depth of field, then this layer of cells lies at the center of the field; half of the field would extend anteriorly where there are no cells and half posteriorly where cell density is lower (Fig. 7, left). This partial filling of the sample volume gives an underestimate of the true cell density in the thin layer, because the use of equation 1 requires that the cells be uniformly distributed through the sample volume.

When the Tandem Scanning microscope is centered on the most anterior keratocytes, its field is also partially filled, but because its depth of field is considerably smaller than that of the ConfoScan 4, less of the field overlaps the anterior region with no cells and the layer just posterior to the stromal surface. The estimated volumetric density would therefore be closer to the true cell density than would the estimates based on the greater depth of field of the ConfoScan 4. The error in density

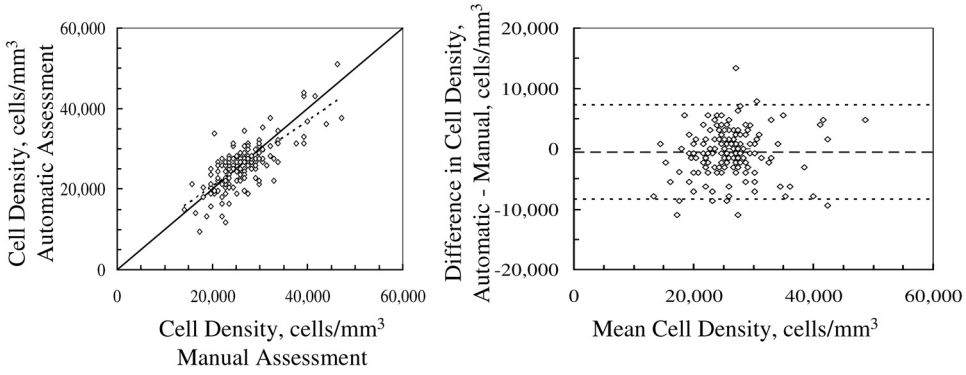

Figure 4. *Left*: the cell density determined by the program in 10 frames from each of 16 normal corneas was correlated with density determined manually in the same frames ($r = 0.81$, $P < 0.001$). *Dashed line*: the regression line; *solid line*: the identity line. *Right*: limits of agreement between the two methods (*fine dashed lines*) were −8336 to 7238 cells/mm^3, by the method of Bland and Altman.[43] The mean difference was −549 cells/mm^3 (*coarse dashed line*).

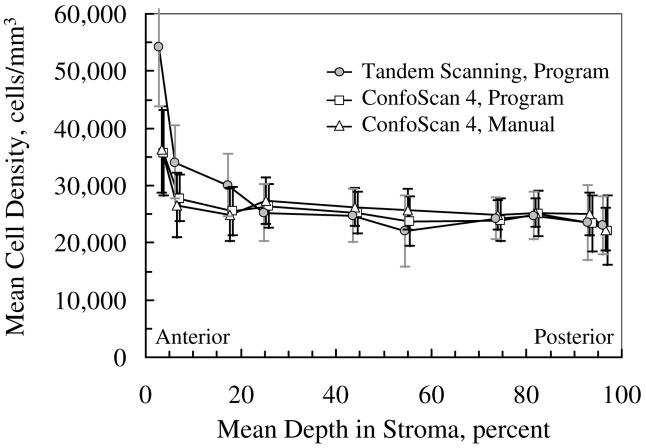

FIGURE 5. Mean cell densities in 16 normal corneas determined by automatic and manual methods in images from the ConfoScan 4 and by automated method from scans by the Tandem Scanning confocal microscope. Densities agreed between instruments in all layers except the anterior 10% of stromal depth. The markers have been offset slightly for clarity. Error bars, ± SD.

estimated by either instrument will depend on the actual distribution of cells through the field of the microscope. The true efficiency of any confocal microscope can be determined only by using an independent measurement of cell density, such as a histologic analysis.[33,42] A narrower depth of field would also show a narrower peak-intensity profile, as the field scans though an edge or a thin layer, as we noted in the scans from the Tandem Scanning microscope (Fig. 6).

The depth of field of confocal microscopes is an important parameter for understanding physical measurements of the cornea and is necessary for calculating the volumetric density of cells in the stroma by this method. This parameter is a characteristic of instrument design and varies with the manufacturer and model. In this study, as in other studies, we measured depth of field directly by scanning through a reflecting surface.[40–42] We added the average thickness of one cell to this parameter to remove bias from counting cells that overlapped the boundaries (analogous to counting cells that overlapped only one edge of the selection rectangle in the plane of the image). This method agrees well with the distance at which cells are visible as the focal plane scans through individual cells.[40] One could also estimate the depth of field of the ConfoScan 4 that forced the mean cell density to be equal to the cell density determined independently—for example, from the Tandem Scanning microscope—if the depth of field of that microscope were known. In our 16 corneas scanned by both instruments, the depth of field that made estimates of cell density equal between instruments was 25.2 ± 1.2 μm, a depth of field close to the 25.4 μm that we measured by scanning through the reflective surface. This method could also be used to estimate depth of field of other confocal microscopes, such as the Heidelberg Retina Tomograph II Rostock Corneal Module (HRT II RCM) confocal laser microscope (Heidelberg Engineering GmbH, Heidelberg, Germany).

Cell Density in Abnormal Corneas

Cell density decreases after LASIK, and the interface created by LASIK scatters more light. Although these corneas are clinically clear, they are not normal by confocal microscopy examination. The similarity between cell densities in the deeper stroma measured by the ConfoScan 4 and the Tandem Scanning confocal microscopes shows that our program worked as well as the program designed to be used with images from the Tandem Scanning microscope. Both instruments and respective programs also detected the subtle, but abnormally low, cell densities near the interface in these subjects, compared with densities in the similar regions of normal corneas. Cell density in the anterior flap was different, however, between the two instruments, and this is consistent with the differences between instruments in the same region of normal corneas. The ConfoScan 4 was not able to detect the density decrease in the anterior flap, although the Tandem Scanning microscope found this difference. This inability is likely a consequence of the greater depth of field and lower sensitivity when estimating volumetric density of cells confined to a thin layer.

Our ability to measure cell density in hazy corneas or corneas with opacities is likely to be limited by the visibility of the cells, and this limitation would affect manual assessment as well as automated assessment. It is prudent to examine frames of potentially abnormal corneas before attempting to assess cell density by either method. For this reason, we routinely selected frames manually for analysis. Selection of suitable frames could be included in the program, although this is a separate step and will require further validation.

Volumetric versus Areal Density

Volumetric density is most appropriate for describing objects such as keratocytes that are distributed through a volume. We and others have reported keratocyte density in volumetric units (cells per cubic millimeter)[1,10,32,33,40,42] whereas other investigators have reported keratocyte density in areal units (cells per square millimeter).[4,5,8,14–16,18,20,34,44–47] A sample of volumetric densities reported in recent papers is given in Table 3, with the reported depths of field of the instrument. Cell densities from these papers were similar to each other and similar to those determined in this study. A small sample of stromal cell densities reported as areal densities is given in Table 4. (Tables 3 and 4 are intended to demonstrate a sample of densities reported recently, but do not serve as a comprehensive review of publications on this topic. For a more complete summary of stromal cell densities reported, see the review by Patel and McGhee.[50]) Cell densities in this sample ranged from 408 to 1057 cells/mm^2, a range of more than a

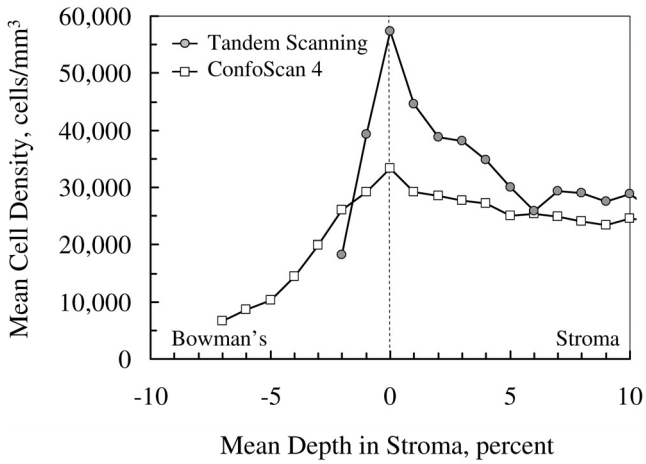

FIGURE 6. Mean cell density in anterior stroma recorded by the ConfoScan 4 and Tandem Scanning confocal microscopes, aligned on the frame with maximum cell density. Maximum cell density was higher and the peak was sharper in scans by the Tandem Scanning microscope, characteristics of its thinner depth of field and the thin, high-density layer of cells in the anterior boundary of the stroma. Cell nuclei appeared in images of the ConfoScan 4 (and increased the apparent density) at a greater distance from their location because of the greater depth of field.

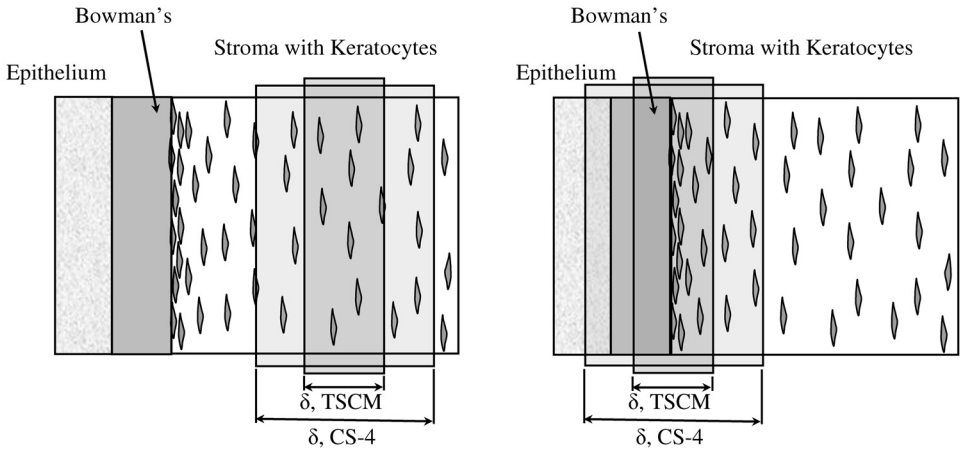

FIGURE 7. Why does the Tandem Scanning confocal microscope show a higher cell density in the anterior stroma than the ConfoScan 4 does? In the deep stroma (*left*), cells were uniformly distributed through the fields of both the ConfoScan 4 and the Tandem Scanning microscopes. However, when the field was focused on the most anterior layer of cells, the cells were distributed though only part of the field (*right*). The field of the ConfoScan 4, which was approximately twice as deep as that of the Tandem Scanning microscope, extended anteriorly so that its anterior half was in Bowman's layer and the epithelium where there were no keratocytes. Cell density, which was calculated by assuming that cells were distributed uniformly throughout the field, was underestimated. The same was true in images from the Tandem Scanning microscope, but because the field depth was only 11.9 μm, the density calculated was closer to true volumetric density.

factor of 2.5. The equivalent volumetric density can be estimated by dividing the areal density by the depth of field reported in the paper plus 1 μm for the cell thickness, by rearranging equation 1. For the sample of papers in Table 4, the estimated volumetric densities ranged from 37,091 to 172,000 cells/mm^3 in the anterior stroma, a considerably greater range and higher densities than the volumetric measurements in Table 3 and those reported by histologic methods. An unrealistic and unreliable estimate of depth of field could explain these differences.

Depths of field vary considerably, depending on the design of the microscope, and have sometimes been specified incorrectly by manufacturers. If we assume a true density of stromal cells for normal corneas, then the depth of field of a particular microscope can be estimated from the areal density. For example, if we assume that the actual cell density in the posterior stroma was 22,166 cells/mm^3, the mean of density in the posterior stroma in Table 3, then the apparent depths of field of the measurements in Table 4 ranged from 14 to 34 μm. In all cases, these were considerably greater than that specified in the paper. When this depth of field was used to estimate volumetric density from the areal density given in the anterior stroma, volumetric densities were closer to those in Table 3. Densities estimated from measurements by Moilanen et al.[49] with the Tandem Scanning confocal microscope and by Niederer et al.[14,47] and Ku et al.[15] with the HRT were greater than the other densities in this region measured by slit-scanning confocal microscopes and were similar to those that we measured in individual frames with the Tandem Scanning confocal microscope. In addition, more cells may be visible in the anterior stroma in these microscopes than they are in the other microscopes. Images of stromal cells in the HRT appear qualitatively brighter and with higher contrast,[50] and this characteristic may make more cell nuclei visible or may make noncellular objects visible that are not visible in other microscopes. This optical difference may make discrimination between keratocytes and other cell types possible, although this capability has not been shown.

Sources of Errors

Several variables may affect the accuracy of manual and automatic assessment of cell density. For example, the cells became less distinct as image brightness diminished. If images were dark enough that an observer could not see the cells, the program also did not detect them. The program worked well unless the mean central field intensity decreased to below approximately 6 iu on the ConfoScan 4, and although we did not have many images at this low intensity, cell densities in these dark images were below what would be expected in a normal stroma. When recording images, the lamp brightness must be set high enough to prevent loss of field intensity. Illumination must not be so high that parts of the image saturate, or clusters of cells will not be separable.

The selection criteria described in Figure 2 were based on one experienced observer. Another observer or the same ob-

TABLE 3. Sample of Studies That Reported Stromal Cell Density in Volumetric Units

Study	Microscope	Depth of Field (μm)	Stromal Cell Density (cells/mm^3 ± SD)		
			Anterior	Midstroma	Posterior
Patel et al.[2]	TSCM	16	28,838 ± 8,913	19,214 ± 2,906	19,947 ± 3,254
Berlau et al.[1]	Microphthal, Hund	10	24,320 ± 6,740	11,610 ± 4,290	18,850 ± 4,610
Popper et al.[42]	Confoscan P-4	9	28,616 ± 5,924	19,578 ± 4,425	26,073 ± 3,077
McLaren et al.[40]	TSCM	11.9		23,013 ± 4,420	
	CS-3	25.9		23,996 ± 2,898	
Kallinikos et al.[10]	CS-3	25.9		29,429 ± 2,232	
Present study	CS-4	25.4	31,677 ± 4,886	24,419 ± 3,498	22,728 ± 4,930
Present study	TSCM	11.9	44,126 ± 6,680	23,317 ± 5,043	23,230 ± 4,798

Microscope manufacturers: Micropthal, Hund, Wetzlar, Germany; Confoscan P-4, Tomey, Erlangen, Germany; CS-3 and CS-4, Nidek Technologies, Padova, Italy; TSCM (Tandem Scanning confocal microscope), Tandem Scanning, Reston, VA.

TABLE 4. Sample of Recent Papers that Reported Cell Density in Areal Units

Reference	Microscope	Reported Depth of Field (μm)	Reported Mean Areal Density (cells/mm^2 ± SD)			Equivalent Mean Volumetric Density (cells/mm^3)			Estimated Depth of Field (μm)	Recalculated Volumetric Density, Anterior (cells/mm^3)
			Anterior	Mid-stroma	Posterior	Anterior	Mid-stroma	Posterior		
Frueh et al.[16]	Microphthal	10	408 ± 71	327 ± 151	413 ± 99	37,091	29,727	38,455	20	20,800
Muston et al.[5]	ConfoScan, P-4	10	1,057 ± 205	*	737 ± 118	96,091	†	67,000	34	30,928
Kallinikos and Efron[9]	ConfoScan, P-4	‡	1,020 ± 397	*	654 ± 147	†	†	†	30	33,139
Vanathi et al.[45]	CS-2	‡	1,005 ± 397	*	654 ± 147	†	†	†	30	33,139
Mocan, et al.[48]	CS-3	‡	1,132 ± 178	770 ± 120	725 ± 113	†	†	†	34	33,671
Moilanen et al.[49]	TSCM	‡	983 ± 178	501 ± 76	390 ± 44	†	†	†	18	54,355
Niederer et al.[14]	HRT II RCM	4	860 ± 219	*	331 ± 52	172,000	†	66,200	15	56,003
Ku et al.[15]	HRT II RCM	4	786 ± 244	*	293 ± 35.3	157,200	†	58,600	14	57,850
Niederer et al.[47]	HRT II RCM	4	765 ± 262	347 ± 64	315 ± 57	153,000	69,400	63,000	15	52,372

The equivalent volumetric densities were calculated by dividing the areal densities by the reported depth of field. The estimated depth of field was calculated by assuming that actual density in the posterior stroma was equal to 22,166 cells/mm^3, the average midstroma and posterior densities given in Table 3. Microscope manufacturers: Micropthal; Hund, Wetzlar, Germany; Confoscan P-4, Tomey, Erlangen, Germany; CS-2 and CS-3, Nidek Technologies, Padova, Italy; TSCM (Tandem Scanning confocal microscope), Tandem Scanning, Reston, VA; HRT II RCM, Heidelberg Engineering, Heidelberg, Germany.

* Midstromal densities not measured.

† Either depth field or areal density not given.

‡ Depth of field not given or assumed.

server on a different occasion might provide somewhat different selection criteria, as demonstrated by McLaren et al.[32] Variations from different observers could introduce differences in mean densities determined from a specific set of scans in a study, and the accuracy of any assessment cannot be determined without using invasive methods. In contrast, the automated program is consistent, if the instrument parameters are not changed. Although there may be small systematic differences between cell density estimated by the program and some observers, the program would be more suitable than multiple observers for assessment of cell density in longitudinal studies. The agreement between the automated assessment of images from the ConfoScan 4 and from the Tandem Scanning confocal microscope in the same corneas suggests that the program extended to the ConfoScan 4 is consistent with the earlier validation on the Tandem Scanning confocal microscope.

Keratocyte nuclei cannot be distinguished from other objects that have similar brightness and contrast and keratocytes cannot be distinguished from other types of cells. The program identified bright objects and selected those that most likely represented cell nuclei, and the selection criteria of this program were determined from images of normal corneas. In pathologic corneas, condensations from scaring or fibrosis that meet the selection criteria will be counted as cells, and in these images, the program may overestimate the cell density. These errors could be avoided by reviewing and selecting frames that show clear, distinct images of cells that are to be assessed. Automatic selection of suitable frames based on image quality is an improvement that could advance the independence and objectivity of this program.

References

1. Berlau J, Becker HH, Stave J, Oriwol C, Guthoff RF. Depth and age-dependent distribution of keratocytes in healthy human corneas: a study using scanning-slit confocal microscopy in vivo. *J Cataract Refract Surg.* 2002;28:611–616.
2. Patel S, McLaren J, Hodge D, Bourne W. Normal human keratocyte density and corneal thickness measurement by using confocal microscopy in vivo. *Invest Ophthalmol Vis Sci.* 2001;42:333–339.
3. Møller-Pedersen T. A comparative study of human corneal keratocyte and endothelial cell density during aging. *Cornea.* 1997;16:333–338.
4. Hollingsworth J, Perez-Gomez I, Mutalib HA, Efron N. A population study of the normal cornea using an in vivo, slit-scanning confocal microscope. *Optom Vis Sci.* 2001;78:706–711.
5. Mustonen RK, McDonald MB, Srivannaboon S, Tan AL, Doubrava MW, Kim CK. Normal human corneal cell populations evaluated by in vivo scanning slit confocal microscopy. *Cornea.* 1998;17:485–492.
6. Efron N, Mutalib HA, Perez-Gomez I, Koh HH. Confocal microscopic observations of the human cornea following overnight contact lens wear. *Clin Exp Optom.* 2002;85:149–155.
7. Efron N, Perez-Gomez I, Morgan PB. Confocal microscopic observations of stromal keratocytes during extended contact lens wear. *Clin Exp Optom.* 2002;85:156–160.
8. Jalbert I, Stapleton F. Effect of lens wear on corneal stroma: preliminary findings. *Aust N Z J Ophthalmol.* 1999;27:211–213.
9. Kallinikos P, Efron N. On the etiology of keratocyte loss during contact lens wear. *Invest Ophthalmol Vis Sci.* 2004;45:3011–3020.
10. Kallinikos P, Morgan P, Efron N. Assessment of stromal keratocytes and tear film inflammatory mediators during extended wear of contact lenses. *Cornea.* 2006;25:1–10.
11. Patel SV, McLaren JW, Hodge DO, Bourne WM. Confocal microscopy in vivo in corneas of long-term contact lens wearers. *Invest Ophthalmol Vis Sci.* 2002;43:995–1003.
12. Hollingsworth JG, Efron N, Tullo AB. In vivo corneal confocal microscopy in keratoconus. *Ophthalmic Physiol Opt.* 2005;25:254–260.
13. Erie JC, Patel SV, McLaren JW, Nau CB, Hodge DO, Bourne WM. Keratocyte density in keratoconus: a confocal microscopy study. *Am J Ophthalmol.* 2002;134:689–695.
14. Niederer RL, Perumal D, Sherwin T, McGhee CNJ. Laser scanning in vivo confocal microscopy reveals reduced innervation and reduction in cell density in all layers of the keratoconic cornea. *Invest Ophthalmol Vis Sci.* 2008;49:2964–2970.
15. Ku JYF, Niederer RL, Patel DV, Sherwin T, McGhee CNJ. Laser scanning in vivo confocal analysis of keratocyte density in keratoconus. *Ophthalmology.* 2008;115:845–850.
16. Frueh BE, Cadez R, Bohnke M. In vivo confocal microscopy after photorefractive keratectomy in humans: a prospective, long-term study. *Arch Ophthalmol.* 1998;116:1425–1431.

17. Møller-Pedersen T, Cavanagh HD, Petroll WM, Jester JV. Stromal wound healing explains refractive instability and haze development after photorefractive keratectomy: a 1-year confocal microscopic study. *Ophthalmology.* 2000;107:1235–1245.
18. Perez-Gomez I, Efron N. Change to corneal morphology after refractive surgery (myopic laser in situ keratomileusis) as viewed with a confocal microscope. *Optom Vis Sci.* 2003;80:690–697.
19. Erie JC, Patel SV, McLaren JW, Hodge DO, Bourne WM. Corneal keratocyte deficits after photorefractive keratectomy and laser in situ keratomileusis. *Am J Ophthalmol.* 2006;141:799–809.
20. Pisella PJ, Auzerie O, Bokobza Y, Debbasch C, Baudouin C. Evaluation of corneal stromal changes in vivo after laser in situ keratomileusis with confocal microscopy. *Ophthalmology.* 2001;108:1744–1750.
21. Bourne WM. Cellular changes in transplanted human corneas. *Cornea.* 2001;20:560–569.
22. Imre L, Resch M, Nagymihaly A. In vivo confocal corneal microscopy after keratoplasty. *Ophthalmologe.* 2005;102:140–146.
23. Patel SV, Erie JC, McLaren JW, Bourne WM. Keratocyte density and recovery of subbasal nerves after penetrating keratoplasty and in late endothelial failure. *Arch Ophthalmol.* 2007;125:1693–1698.
24. Mikek K, Hawlina M, Pfeifer V. Comparative study of human keratocyte density after corneal grafting by using confocal microscopy in vivo. *Klin Monatsbl Augenheilkd.* 2003;220:830–834.
25. Patel SV, McLaren JW, Hodge DO, Bourne WM. The effect of corneal light scatter on vision after penetrating keratoplasty. *Am J Ophthalmol.* 2008;146:913–919.
26. Masters BR, Bohnke M. Three-dimensional confocal microscopy of the living human eye. *Ann Rev Biomed Eng.* 2002;4:69–91.
27. Böhnke M, Masters BR. Confocal microscopy of the cornea. *Prog Retin Eye Res.* 1999;18:553–628.
28. Hamrah P, Dana MR. Corneal antigen-presenting cells. *Chem Immunol Allergy.* 2007;92:58–70.
29. Yamagami S, Ebihara N, Usui T, Yokoo S, Amano S. Bone marrow-derived cells in normal human corneal stroma. *Arch Ophthalmol.* 2006;124:62–69.
30. Yamagami S, Usui T, Amano S, Ebihara N. Bone marrow-derived cells in mouse and human cornea. *Cornea.* 2005;24:S71–S74.
31. Hamrah P, Huq SO, Liu Y, Zhang Q, Dana MR. Corneal immunity is mediated by heterogeneous population of antigen-presenting cells. *J Leukoc Biol.* 2003;74:172–178.
32. McLaren JW, Patel SV, Nau CB, Bourne WM. Automated assessment of keratocyte density in clinical confocal microscopy of the corneal stroma. *J Microsc.* 2008;229:21–31.
33. Patel SV, McLaren JW, Camp JJ, Nelson LR, Bourne WM. Automated quantification of keratocyte density by using confocal microscopy in vivo. *Invest Ophthalmol Vis Sci.* 1999;40:320–326.
34. Prydal JI, Franc F, Dilly PN, Kerr Muir MG, Corbett MC, Marshall J. Keratocyte density and size in conscious humans by digital image analysis of confocal images. *Eye.* 1998;12:337–342.
35. McLaren JW, Nau CB, Patel SV, Bourne WM. Measuring corneal thickness with the ConfoScan 4 and z-ring adapter. *Eye Contact Lens.* 2007;33:185–190.
36. Patel SV, Maguire LJ, McLaren JW, Hodge DO, Bourne WM. Femtosecond laser versus mechanical microkeratome for LASIK: a randomized controlled study. *Ophthalmology.* 2007;114:1482–1490.
37. McLaren JW, Nau CB, Erie JC, Bourne WM. Corneal thickness measurement by confocal microscopy, ultrasound, and scanning slit methods. *Am J Ophthalmol.* 2004;137:1011–1020.
38. Erie JC, Nau CB, McLaren JW, Hodge DO, Bourne WM. Long-term keratocyte deficits in the corneal stroma after LASIK. *Ophthalmology.* 2004;111:1356–1361.
39. Mitooka K, Ramirez M, Maguire LJ, et al. Keratocyte density of central human cornea after laser in situ keratomileusis. *Am J Ophthalmol.* 2002;133:307–314.
40. McLaren JW, Nau CB, Kitzmann AS, Bourne WM. Keratocyte density: comparison of two confocal microscopes. *Eye Contact Lens.* 2005;31:28–33.
41. Petroll WM, Cavanagh HD, Jester JV. Three-dimensional imaging of corneal cells using in vivo confocal microscopy. *J Microsc.* 1993;170:213–219.
42. Popper M, Morgado AM, Quadrado MJ, Van Best JA. Corneal cell density measurement in vivo by scanning slit confocal microscopy: method and validation. *Ophthalmic Res.* 2004;36:270–276.
43. Bland JM, Altman DG. Statistical methods for assessing agreement between two methods of clinical measurement. *Lancet.* 1986;1:307–310.
44. Møller-Pedersen T. Corneal keratocyte density: aspects of methodology, physiology and pathophysiology. *Acta Ophthalmol Scand.* 1999;77:366–367.
45. Vanathi M, Tandon R, Sharma N, Titiyal JS, Pandey RM, Vajpayee RB. In-vivo slit scanning confocal microscopy of normal corneas in Indian eyes. *Indian J Ophthalmol.* 2003;51:225–230.
46. Vesaluoma M, Perez-Santonja J, Petroll WM, Linna T, Alio J, Tervo T. Corneal stromal changes induced by myopic LASIK. *Invest Ophthalmol Vis Sci.* 2000;41:369–376.
47. Niederer RL, Perumal D, Sherwin T, McGhee CNJ. Age-related differences in the normal human cornea: a laser scanning in vivo confocal microscopy study. *Br J Ophthalmol.* 2007;91:1165–1169.
48. Mocan M, Yilmaz P, Irkec M, Orhan M. In vivo confocal microscopy for the evaluation of corneal microstructure in keratoconus. *Curr Eye Res* 2008;33:933–939.
49. Moilanen JAO, Holopainen JM, Vesaluoma MH, Tervo TMT. Corneal recovery after LASIK for high myopia: a 2-year prospective confocal microscopic study. *Br J Ophthalmol.* 2008;92:1397–1402.
50. Patel DV, McGhee CNJ. Contemporary in vivo confocal microscopy of the living human cornea using white light and laser scanning techniques: a major review. *Clin Exp Ophthalmol.* 2007;35:71–88.